VIROLOGY

CCR2 is a host entry receptor for severe fever with thrombocytopenia syndrome virus

Leike Zhang[1,2]†, Xuefang Peng[3]†, Qingxing Wang[1]†, Jin Li[4]†, Shouming Lv[3], Shuo Han[3], Lingyu Zhang[3], Heng Ding[3], Cong-Yi Wang[5], Gengfu Xiao[1], Xuguang Du[4], Ke Peng[1]*, Hao Li[3,6]*, Wei Liu[3,6]*

Severe fever with thrombocytopenia syndrome virus (SFTSV) is an emerging tick-borne bunyavirus causing a high fatality rate of up to 30%. To date, the receptor mediating SFTSV entry remained uncharacterized, hindering the understanding of disease pathogenesis. Here, C-C motif chemokine receptor 2 (CCR2) was identified as a host receptor for SFTSV based on a genome-wide CRISPR-Cas9 screen. Knockout of CCR2 substantially reduced viral binding and infection. CCR2 enhanced SFTSV binding through direct binding to SFTSV glycoprotein N (Gn), which is mediated by its N-terminal extracellular domain. Depletion of CCR2 in C57BL/6J mouse model attenuated SFTSV replication and pathogenesis. The peripheral blood primary monocytes from elderly individuals or subjects with underlying diabetes mellitus showed higher CCR2 surface expression and supported stronger binding and replication of SFTSV. Together, these data indicate that CCR2 is a host entry receptor for SFTSV infection and a novel target for developing anti-SFTSV therapeutics.

INTRODUCTION

Emerging arboviral diseases pose a serious threat to public health and global economy. The World Health Organization (WHO) recently launched the Global Arbovirus Initiative to raise the global alarm on the risk of epidemics of arboviruses and the potential risk of pandemics (*1*). Several different families of arboviruses, including phenuiviruses, nairoviruses, and hantaviruses, can cause viral hemorrhagic fever (VHF) in humans. Severe fever with thrombocytopenia syndrome (SFTS) caused by a bunyavirus [SFTS virus (SFTSV)] that was recently named Dabie bandavirus in the family Phenuiviridae (formerly Bunyaviridae) is the most notorious VHF disease, primarily because of its wide geographical distribution and high mortality rate (12 to 50%). Since its first identification in China in 2009 (*2*), SFTS has affected a rapidly growing number of people, with a consistently expanded geographic distribution, mostly in Asian countries, including China, Korea, Japan, Vietnam, Pakistan, Myanmar, and Thailand (*3*–*10*).

Tick-to-human transmission is the main route by which people are infected with SFTSV, and *Hemaphysalis longicornis* is the predominant tick vector (*11*). This tick species, originally native to East and Southeast Asia and eastern Russia, spread to Australia and Western Pacific regions more than 200 years ago (*12*) and was recently found in the eastern United States (*13*). Cases of human-to-human transmission through exposure to blood or bloody secretions of SFTS patients have been increasingly reported (*14*). The escalating numbers of human patients, the rapid spread of tick vectors worldwide, and the multiple occurrences of human-to-human transmission cases have raised concern about the potential SFTS pandemic, promoting the prioritized research declaration on SFTS by the WHO (*15*).

Resembling the clinical syndrome manifested in VHF, SFTSV infection results in severe or critical consequences, including hemorrhage, encephalitis, and multiple organ failure, all of which are related to high probability of death, ranging from 16.2% in China to 23.3% in South Korea and 27.0% in Japan (*5*, *16*–*18*). Despite the clinical significance, specific therapeutics against SFTS are unavailable, in part due to the lack of knowledge on host factors, especially the cellular entry receptors, that contribute to SFTSV infection.

SFTSV is a negative-sense single-stranded RNA (ssRNA) virus and contains a segmented, tripartite genome of large (L), medium (M), and small (S) segments. The M segment encodes a glycoprotein precursor (Gp) that is processed into two subunits: glycoprotein N (Gn) and glycoprotein C (Gc). Resembling Rift Valley fever virus (RVFV), another highly lethal member in the family Phenuiviridae (*19*, *20*), the Gc protein of SFTSV is a class II fusion protein (*21*), and the Gn protein of SFTSV plays a key role in receptor binding by serving as "spikes" on the virion surface (*21*, *22*). Currently, only a few attachment factors and receptors are known for phenuiviruses. The glycosaminoglycan heparan sulfate (HS) has been indicated as an attachment factor for RVFV and Toscana virus (TOSV) (*23*). The C-type lectin dendritic cell–specific intercellular adhesion molecule-3–grabbing nonintegrin (DC-SIGN) has been recognized as an endocytic factor for RVFV, SFTSV, and Uukuniemi virus (UUKV) (*24*–*26*). The role of these host factors in disease pathogenesis and their clinical relevance have rarely been disclosed. Phenuiviruses may use multiple receptors to target and infect abundant numbers of distinct cell types, tissues, and species (*20*), and many aspects of phenuivirus receptors thus remain to be studied. High-throughput screens by selectively inactivating genes of the human genome are conducive to identifying novel factors essential for cellular entry by phenuiviruses. For example, by using the

[1]State Key Laboratory of Virology, Wuhan Institute of Virology, Chinese Academy of Sciences, Wuhan, Hubei 430071, China. [2]Hubei Jiangxia Laboratory, Wuhan, Hubei 430200, China. [3]State Key Laboratory of Pathogen and Biosecurity, Beijing Institute of Microbiology and Epidemiology, Beijing 100071, China. [4]State Key Laboratory of Agrobiotechnology, College of Biological Sciences, China Agricultural University, Beijing 100193, China. [5]Tongji Hospital, Tongji Medical College, Huazhong University of Science and Technology, Wuhan, Hubei 430040, China. [6]School of Public Health, Wuhan University, Wuhan, Hubei 430071, China.
*Corresponding author. Email: lwbime@163.com (W.L.); lihao_1986@126.com (H.L.); pengke@wh.iov.cn (K.P.)
†These authors contributed equally to this work.

CRISPR-Cas9 system, low-density lipoprotein receptor–related protein 1 (LRP1) was identified as a host entry factor for RVFV and suggested as a new target to limit RVFV infections (*20*).

Here, by performing a genome-wide CRISPR-Cas9–based screen, we identified C-C motif chemokine receptor 2 (CCR2), a G protein–coupled receptor (GPCR), as a critical host factor for SFTSV entry. Knockout (KO) of CCR2 markedly reduced SFTSV infection in cells, while overexpression of CCR2 resulted in increased infection. A direct interaction between SFTSV Gn and the N-terminal extracellular domain of CCR2, mediated by tyrosine sulfation at the Y26 site, was further demonstrated. The disruption of the interaction process inhibited virus binding otherwise. The significance of the Gn-CCR2 interaction was validated in mouse models through protection against SFTSV lethal infection through CCR2 deletion or CCR2 antagonist treatment. Clinical significance was displayed in that peripheral blood primary human monocytes from elderly individuals or subjects with underlying diabetes mellitus (DM) expressed higher levels of CCR2 and supported stronger SFTSV entry and replication, thus uncovering why these individuals are at higher risk for lethal SFTSV infection.

RESULTS

Genome-wide CRISPR-Cas9–based screening identified CCR2 as a critical factor for SFTSV infection

To identify cellular factors required for SFTSV infection, we performed a genome-wide *piggyBac* (PB)–CRISPR/Cas9–based screen using the GeCKOv2 library in Huh7 cells (*27*, *28*). We used an authentic SFTSV strain isolated from a febrile patient to infect the library-transduced cells and wild-type (WT) cells at a multiplicity of infection (MOI) of 5 for 48 hours. Approximately 10% uninfected cells as determined by fluorescence-activated cell sorting with the use of a rabbit polyclonal antibody against SFTSV nucleoprotein (NP) were enriched from the library-transduced cells, while the WT Huh7 cells showed efficient infection (fig. S1). The SFTSV-negative cells were subjected to single-guide RNA (sgRNA) amplification and next-generation sequencing. CCR2, which is a member of the class A GPCRs and the key functional receptor for monocyte chemoattractant protein 1/chemokine ligand 2 (CCL2) (*29*), was identified as one of the top hits of all the membrane proteins (table S1).

The role of CCR2 in SFTSV infection was first validated by RNA interference. In Huh7 cells, knockdown of CCR2 showed a stronger inhibitory effect on SFTSV infection than silencing of activating transcription factor 6 (ATF6), an important host factor for maintaining the intracellular level of SFTSV Gp and virus replication (*30*), which was included as a positive control (fig. S2, A and B). CCR2 is expressed on monocytes and macrophages, both of which act as the target cells of SFTSV infection in human patients and mouse models (*31*, *32*). Silencing CCR2 in THP-1 cells, a human monocytic cell line, and Raw264.7 cells, a murine monocytic cell line, also reduced SFTSV infection by up to 60 and 50%, respectively (Fig. 1, A to C, and fig. S2, C and D). We further generated *CCR2*-KO THP-1 cells using the CRISPR-Cas9 system, for which both gene deletion and cell viability were confirmed (fig. S3, A to D). Infection of four authentic SFTSV strains, representative of phylogenetically distinct clades that circulate in human patients (*33*, *34*), was strongly inhibited in *CCR2*-KO THP-1 cells, with intracellular viral RNA (vRNA) levels reduced by more than 80% (Fig. 1D). Notably, the production of SFTSV progeny virions was reduced by nearly 1000 times in *CCR2*-KO cells at 72 hours after virus inoculation (Fig. 1E). Next, bone marrow–derived macrophages (BMDMs) were prepared from $CCR2^{-/-}$ and WT C57BL/6J mice and subsequently subjected to assessment of SFTSV infectivity (Fig. 1F). Compared to the BMDMs isolated from WT controls, the production of SFTSV progeny virions was significantly reduced in the cells from $CCR2^{-/-}$ mice (Fig. 1, G and H). The inhibitory effect on SFTSV infection was further confirmed by immunostaining of intracellular SFTSV NP in BMDMs from $CCR2^{-/-}$ mice (Fig. 1I).

CCR2 exists as two splice variants, named CCR2A and CCR2B, which differ only in the lengths of their C termini (*29*). The lentivirus-mediated overexpression of CCR2A and CCR2B was conducted in Huh7, HeLa, and Jurkat cells with relatively low CCR2 surface expression levels (fig. S3E), which resulted in significantly increased SFTSV infection rates and viral titers in all three cell lines (Fig. 1, J to L, and fig. S4). Notably, overexpression of CCR2B, the predominant isoform of the CCR2 surface receptors (*35*), showed a stronger impact on promoting SFTSV infection than overexpression of CCR2A (Fig. 1, J to L). Together, these results demonstrate that CCR2 is a critical host factor for SFTSV infection in vitro.

Effect of CCR2 inhibitors and antibody on SFTSV infection in cells

Two small-molecule inhibitors specific for CCR2, antagonist RS102895 and antagonist 1, which can potently compete against CCL2 binding to CCR2, were used to pretreat THP-1 or Huh7 cells before the inoculation of SFTSV. At 24 hours after infection, CCR2 antagonist RS102895 and antagonist 1 significantly inhibited SFTSV infection by detecting the intracellular SFTSV vRNA levels and supernatant viral titers, when oseltamivir phosphate and benidipine hydrochloride were used as the negative and positive controls, respectively (fig. S5, A to D). Moreover, both CCR2 antagonists showed a dose-dependent inhibitory effect on SFTSV infection in THP-1 and Huh7 cells (Fig. 2, A to F, and fig. S5, E and F). The half cytotoxic concentration (CC_{50}) and half maximal inhibitory concentration (IC_{50}) were determined to be 101.7 and 3.061 μM for CCR2 antagonist RS102895 and 4150 and 37.76 μM for CCR2 antagonist 1 in Huh7 cells, resulting in selection indices of 33.2 and 109.9, respectively (Fig. 2, D and E). Consistently, incubation with an anti-human CCR2 antibody also inhibited the production of SFTSV progeny virions in THP-1 cells in a dose-dependent manner (Fig. 2G). SFTSV infection rates measured by flow cytometry analysis were significantly reduced in cells treated with the anti-human CCR2 antibody at MOIs of 1 and 5 (Fig. 2, H and I). These findings suggest that inhibitors and antibodies targeting CCR2 present potential therapeutic avenues to treat SFTS.

CCR2 is essential for SFTSV binding

CCR2 is a GPCR localized on the plasma membrane and has been recognized as a co-receptor for HIV-1 (*36*); thus, we analyzed whether it might function in SFTSV entry. Compared with infection of BMDMs isolated from WT C57BL/6J mice, SFTSV binding and internalization were significantly reduced by approximately 60 and 80%, respectively, in $CCR2^{-/-}$ BMDMs (Fig. 3, A and B). This effect on viral binding was further supported by an immunofluorescence assay detecting cell-bound SFTSV NP protein (Fig. 3C). The binding of SFTSV was also reduced by approximately 40% in

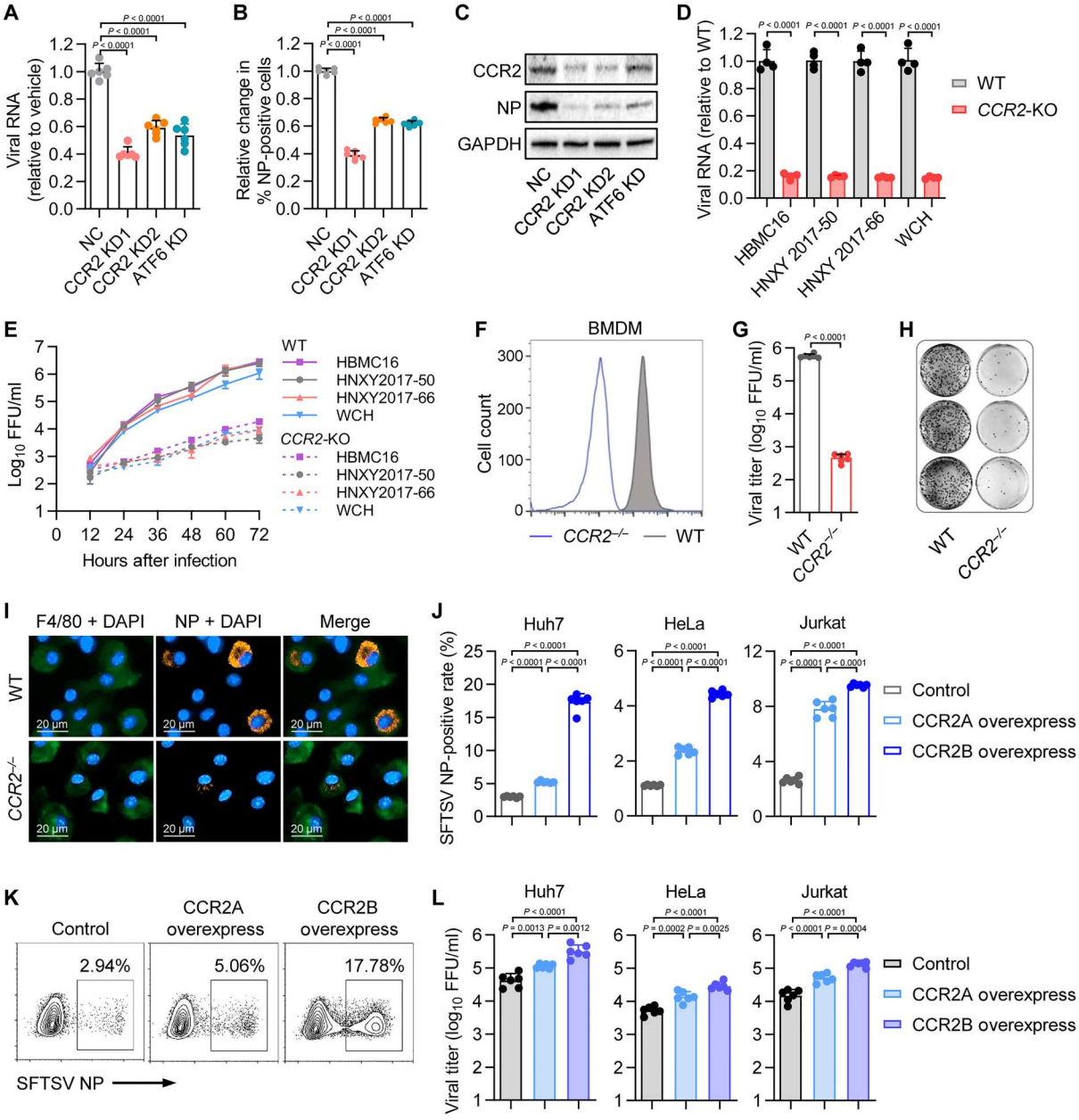

Fig. 1. CCR2 is required for efficient SFTSV infection in cells. (**A** to **C**) RT-qPCR (A), flow cytometry (B), and Western blot (C) analysis of SFTSV infection at 24 hours after infection in CCR2- or ATF6-knockdown THP-1 cells. $n = 6$. GAPDH, glyceraldehyde-3-phosphate dehydrogenase. (**D**) RT-qPCR analysis of virus RNA in CCR2-KO THP-1 cells inoculated with four phylogenetically distinct SFTSV strains, including HBMC16, HNXY2017-50, HNXY2017-66, and WCH, for 24 hours. $n = 4$. (**E**) Multistep growth curves of four SFTSV strains in CCR2-KO THP-1 cells. $n = 4$. (**F**) Surface expression of CCR2 on BMDMs from *CCR2*$^{-/-}$ and WT C57BL/6J mice. A representative of three replicates is shown. (**G** and **H**) Statistical results (G) and scanned images (H) of the immunological focus assay of SFTSV titers at 24 hours after infection in BMDMs with deletions in CCR2. $n = 6$. (**I**) Microscopy of BMDMs immunostained for F4/80, SFTSV NP, and DAPI at 24 hours after infection. (**J**) SFTSV infection rates at 24 hours after infection determined by flow cytometry analysis in Huh7, HeLa, and Jurkat cells overexpressing CCR2A or CCR2B. $n = 6$. (**K**) Representative flow plot of SFTSV infection in Huh7 cells. (**L**) Supernatant viral titers measured by immunological focus assay in Huh7, HeLa, and Jurkat cells overexpressing CCR2A or CCR2B. $n = 6$. Two-tailed Student's *t* test was performed for comparison of variables between two groups [(A), (B), (D), and (G)]. One-way ANOVA followed by Tukey's multiple comparisons test was performed for comparison of variables among three groups [(J) and (K)].

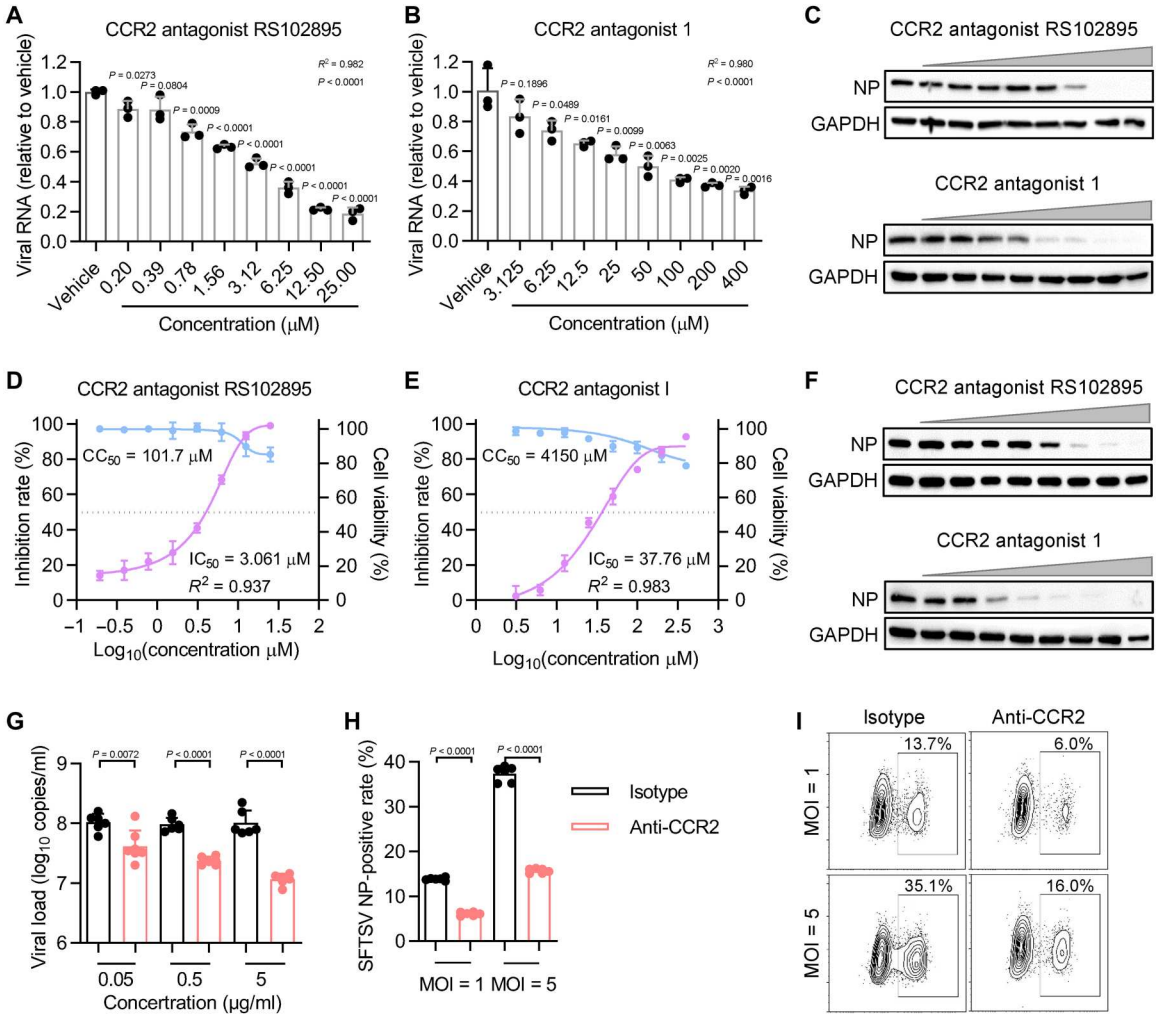

Fig. 2. Effect of CCR2 inhibitor and antibody on SFTSV infection in cells. (**A** to **F**) Effects of CCR2 antagonist RS102895 and CCR2 antagonist 1 on SFTSV infection in THP-1 (A) to (C) and Huh7 cells (D) to (F). At 24 hours after infection, relative vRNA levels were measured via RT-qPCR [(A), (B), (D), and (E), $n = 3$], and relative intracellular SFTSV NP levels were measured by Western blotting (C) and (F). Cell viability was measured using CCK-8 [(D) and (E), $n = 3$]. (**G** to **I**) Effects of CCR2 antibody on SFTSV infection in THP-1 cells. The dose-dependent inhibitory effects of the CCR2 antibody were analyzed by detecting virus loads in THP-1 cells at 24 hours after infection [(G), $n = 6$]. SFTSV infection rates were measured at 24 hours after infection with MOIs of 1 and 5 [(H), $n = 6$]. Representative flow plot of SFTSV infection in THP-1 cells treated with anti-human CCR2 or isotype control antibody (I). Two-tailed Student's t test was performed for comparison of variables between two groups [(A), (B), (D), (E), (G), and (H)]. R^2 [(A), (B), (D), and (E)] was estimated by a nonlinear regression model (curve fit).

CCR2-KO THP-1 cells (Fig. 3, D and E). Reciprocally, overexpression of CCR2A or CCR2B enhanced SFTSV binding in Huh7, HeLa, and Jurkat cells, of which CCR2B (1.6- to 2.6-fold increase) showed a stronger effect in promoting SFTSV binding than CCR2A (1.3- to 1.6-fold increase) (Fig. 3F). Treatment with two CCR2 antagonists significantly inhibited SFTSV binding and internalization, while favipiravir, a known anti-SFTSV drug that inhibits viral genome replication (*37*), did not show such an effect (Fig. 3, G to I, and fig. S6). We additionally inoculated *CCR2*-KO THP-1 cells with a panel of bunyaviruses that are pathogenic to human beings, i.e., Heartland virus (HRTV), RVFV, or Amur hantavirus (AMRV), but revealed no significantly reduced effect on viral binding (Fig. 3J). The CCR2 antagonists also did not affect the binding of these bunyaviruses to THP-1 cells (Fig. 3, K and L). These results together suggest that CCR2 may act as a specific host entry factor for SFTSV.

The N-terminal domain of CCR2 directly binds to the SFTSV virion

To analyze the physical interaction between SFTSV and CCR2, we performed coimmunoprecipitation assay. We confirmed the interaction between SFTSV Gn and both CCR2 isoforms (CCR2A and CCR2B), but not between SFTSV Gn and enhanced green fluorescent protein (EGFP) or membrane protein scavenger receptor class B member 1 (SCARB1), which served as negative controls (Fig. 4A). CCR2A and CCR2B have a common N-terminal extracellular domain, which mediates ligand binding to CCL2 (*29*); thus, the effect of the CCR2 N-terminal extracellular domain on the infectivity of SFTSV was further assessed. The CCR2 construct in which the N-terminal region was deleted without affecting the expression of CCR2 on the cell surface (fig. S7) showed no promoting effect on SFTSV infection in five cell lines, i.e., Huh7, HeLa, Jurkat, NALM-6, and HL-7702 cells (Fig. 4, B to F, and fig. S8A). In the extracellular

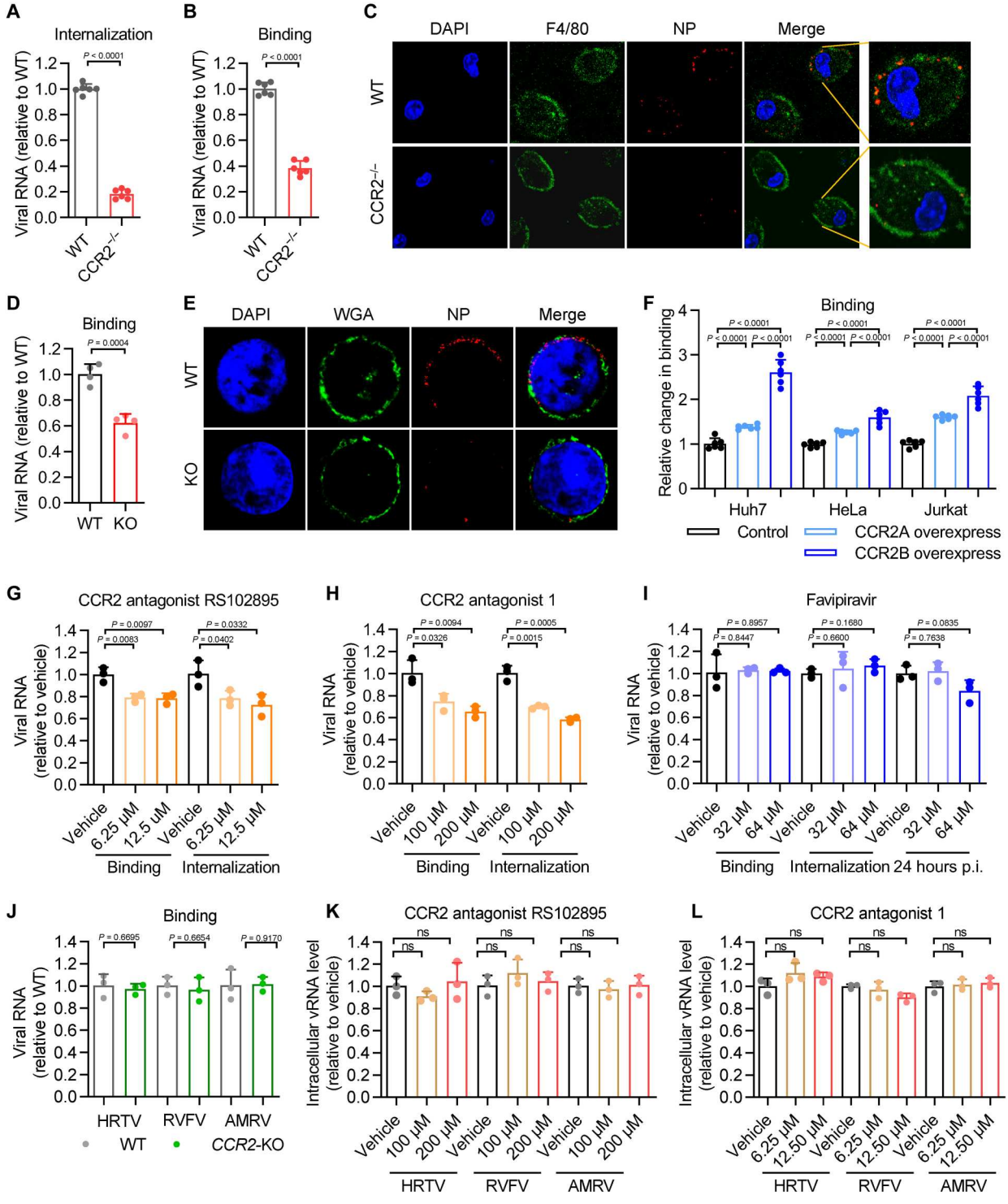

Fig. 3. CCR2 mediates SFTSV binding and internalization. (**A** and **B**) Effects of CCR2 deletions on the internalization (A) and binding (B) of SFTSV in BMDMs. Relative vRNA levels were measured via RT-qPCR. $n = 6$. (**C**) Fluorescence microscopy analysis of the effects of CCR2 deletions on the binding of SFTSV. BMDMs were immunostained with F4/80 (green), SFTSV NP (red), and DAPI. A representative of three replicates is shown. (**D** and **E**) SFTSV binding assay in CCR2-KO (KO) THP-1 cells by using RT-qPCR (D) and immunofluorescence staining (E). $n = 4$. Cellular membranes were labeled with WGA. (**F**) Flow cytometry analysis of SFTSV infection at 2 hours after infection in Huh7, HeLa, and Jurkat cells overexpressing CCR2A or CCR2B. $n = 6$. (**G** to **I**) Effects of the CCR2 antagonist RS102895 (G), CCR2 antagonist 1 (H), and favipiravir (I) on the binding and internalization of SFTSV in THP-1 cells. $n = 3$. (**J**) Binding assay of HRTV, RVFV, and AMRV for control and CCR2-KO THP-1 cells. $n = 3$. (**K** and **L**) Effects of CCR2 antagonist RS102895 (K) and CCR2 antagonist 1 (L) on the binding of HRTV, RVFV, and AMRV in THP-1 cells. $n = 3$. Two-tailed Student's t test was performed for comparison of variables between two groups [(A), (B), (D), and (J)]. One-way ANOVA followed by Tukey's multiple comparisons test was performed for comparison of variables among three groups [(F) to (I), (K), and (L)]. ns, no significance; p.i., post-infection.

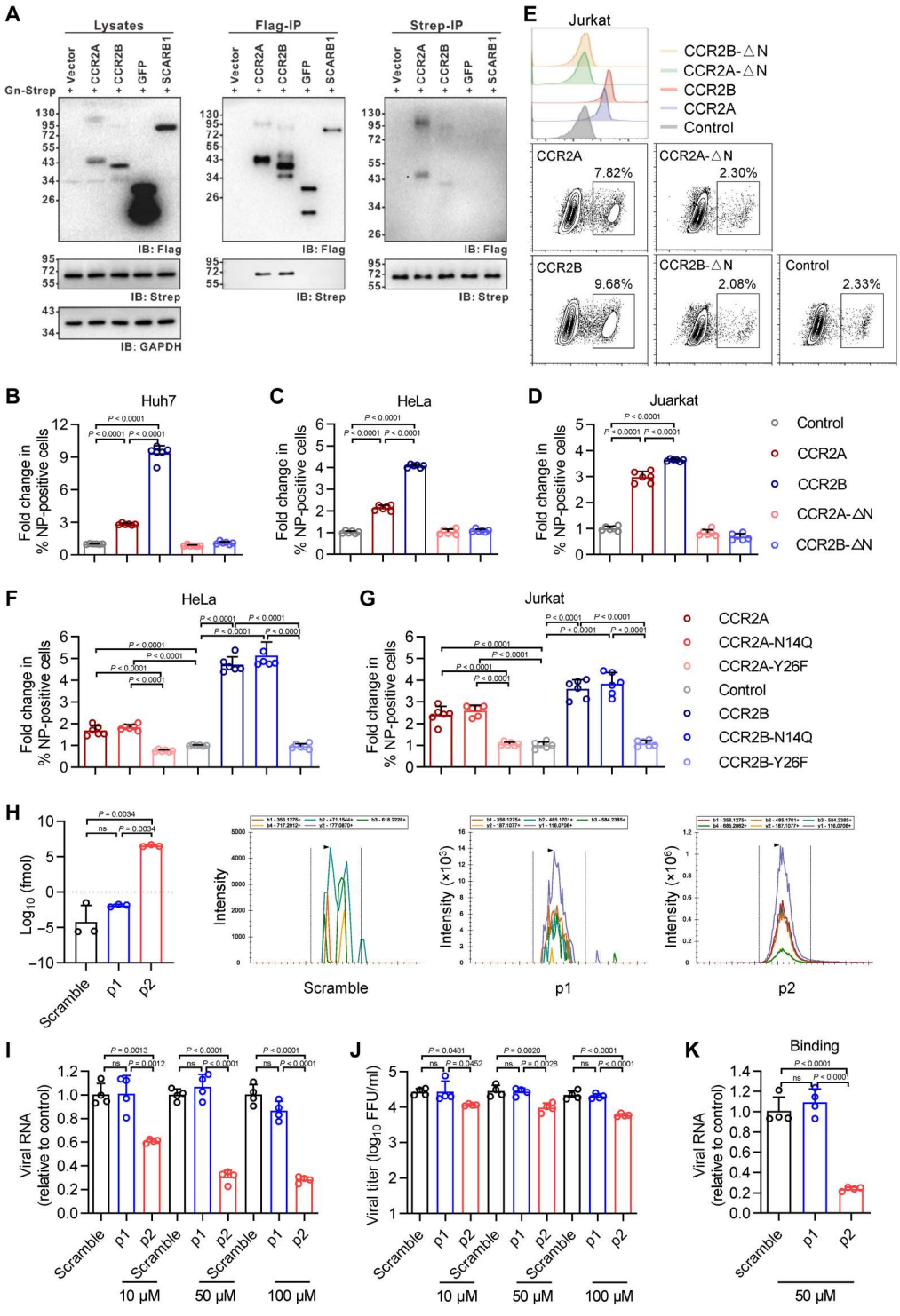

Fig. 4. The CCR2 N-terminal extracellular domain mediates SFTSV binding to cells. (**A**) Coimmunoprecipitation of co-overexpressed Gn-strep protein and CCR2-flag proteins in HEK293T cells using strep-tag binding beads or anti-Flag antibody beads. Vector-flag, GFP-flag, and SCARB1-flag proteins were used as negative controls. (**B** to **D**) Effect of CCR2 overexpression on the infectivity of SFTSV in Huh7 (B), HeLa (C), and Jurkat (D) cells. SFTSV infection rates were measured at 24 hours after infection by flow cytometry analysis in control-, CCR2A-, CCR2B-, CCR2A-ΔN–, and CCR2B-ΔN–overexpressing cells. $N = 6$. (**E**) Surface expression of CCR2 and representative flow plot of SFTSV infection in Jurkat cells. (**F** and **G**) Effect of the CCR2 N-terminal extracellular domain on the infectivity of SFTSV in HeLa (F) and Jurkat (G) cells. SFTSV infection rates were measured at 24 hours after infection by flow cytometry in control-, CCR2A-, CCR2A-N14Q–, CCR2A-Y26F–, CCR2B-, CCR2B-N14Q–, and CCR2B-Y26F–overexpressing cells. $n = 6$. (**H**) Binding of CCR2 N-terminal–derived Y26 sulfated peptide (p2), peptide without tyrosine sulfation at Y26 (p1), or the scrambled peptide to SFTSV virions determined by PRM assay. Statistical analysis is shown in the left panel, and PRM transitions are shown in the right panel. (**I** and **J**) Effect of CCR2 N-terminal–derived peptides on the infectivity of SFTSV in THP-1 cells. Relative intracellular vRNA levels and supernatant viral titers were measured at 24 hours after infection via RT-qPCR. $n = 4$. (**K**) Effect of CCR2 N-terminal–derived peptides on the binding of SFTSV in THP-1 cells. Relative levels of bound virions were measured via RT-qPCR. $n = 4$. One-way ANOVA followed by Tukey's multiple comparisons test was performed for comparison of variables among three groups [(B) to (D) and (F) to (K)].

N-terminal domain of CCR2, Y26 is recognized as a tyrosine sulfation site that plays an important role in ligand binding (*38*, *39*). The Y to F substitution at this site (Y26F) impaired CCR2′s capacity to promote SFTSV binding and infection (Fig. 4, F and G, and fig. S8B). In contrast, a mutant construct with N to Q substitution in N14 (N14Q), a glycosylation site that has no impact upon ligand binding to CCR2 (*36*, *40*), supported SFTSV infection in HeLa and Jurkat cells similar to WT CCR2 (Fig. 4, F and G).

To determine whether SFTSV directly binds to the CCR2 N-terminal domain, we incubated purified SFTSV virions together with equal amounts of peptides derived from the N-terminal region of CCR2 (*18*–*31*) and then performed immunoprecipitation (IP) with an MAb4-5 antibody, which specifically recognizes the

SFTSV Gn protein (*21*). The absolute quantification of SFTSV-bound peptides was further evaluated by using a parallel reaction monitoring (PRM) assay, a targeted mass spectrometry (MS) method that has been widely used to quantify peptides (*41*). CCR2 N-terminal–derived Y26 sulfated peptide (p2) was enriched by SFTSV virions, which was not observed for the peptide without tyrosine sulfation at Y26 (p1) or the scrambled peptide (Fig. 4H and fig. S9). Moreover, pretreatment of SFTSV virions with the sulfated peptide p2 markedly reduced SFTSV infection in a dose-dependent manner (Fig. 4, I and J) and significantly blocked viral binding (Fig. 4K). In contrast, neither the nonsulfated peptide p1 nor the scrambled peptide showed an inhibitory effect on SFTSV infection. These results suggest that the sulfated peptide p2 exclusively interacts with SFTSV virions in a direct manner.

CCR2 is required for lethal SFTSV infection in mouse models

We next sought to evaluate the effect of CCR2 on SFTSV infection and disease pathogenesis in mouse models. In the SFTSV-infected C57BL/6J mouse model (*32*), we observed significantly decreased viral loads in the serum and spleen samples of *CCR2*$^{-/-}$ mice at 3 and 5 days after intraperitoneal challenge with SFTSV (Fig. 5A). In the SFTSV-infected lethal mouse model enabled through pretreatment with anti–interferon α receptor 1 (IFNAR1) immunoglobulin G (IgG) antibody that can recapitulate human clinical symptoms (*42*), we observed a faster recovery in body weight with significant increases at 5 to 9 days post-infection (dpi) (all $P < 0.05$; Fig. 5B), and a significantly enhanced survival rate (by 55%: from 64 to 9%, $P = 0.0060$) in *CCR2*$^{-/-}$ mice (Fig. 5B). In the WT control group, death occurred at 5 ($n = 3$), 6 ($n = 3$), and 7 ($n = 1$) dpi, resulting in an average survival time (AST) of 5.7 days. Notably, significantly increased AST was observed for the *CCR2*$^{-/-}$ (7 days) mice that succumbed to infection (Fig. 5C). To analyze the effect of CCR2 on viremia, viral dissemination, and tissue pathology, four mice from each group were euthanized at 3 and 5 dpi. The viral titers in the serum, spleen, liver, and lung samples were all inhibited (Fig. 5D), and the reduced SFTSV infection was verified in the spleen, liver, and lung tissues with immunohistochemistry (Fig. 5E). *CCR2*$^{-/-}$ mice with SFTSV infection showed alleviated pathogenesis in comparison with the WT control, as evidenced by attenuated histopathological abnormalities, e.g., white pulp atrophy and increased megakaryocyte counts in the spleen, coagulation necrosis and mononuclear cell infiltration in the liver, and widening of the alveolar septum and interstitial infiltrates in the lung (Fig. 5F). In addition, using the anti-IFNAR1 antibody–pretreated C57BL/6J mouse model, CCR2 antagonist treatment also significantly reduced the viral loads in the serum, spleen, and liver samples (Fig. 5F and fig. S10A) and markedly alleviated SFTSV-induced pathogenesis (fig. S10B), compared to vehicle control. In the vehicle control group, SFTSV infection led to the fatality rate of 61.5% (8 of 13) and CCR2 antagonist treatment significantly decreased the fatality rate to 23.1% (3 of 13, $P = 0.0218$; Fig. 5H). These in vivo experiments establish a function for CCR2 in the pathogenesis of SFTSV infection.

CCR2 contributes to severe SFTSV infection in the patients

SFTS patients with older age or preexisting comorbidities, particularly DM, have been demonstrated to be at a higher risk for fatal outcomes (*5*, *6*, *43*); however, the underlying mechanism is obscure. Considering the well-acknowledged increased expression of CCR2 on monocytes in the elderly and individuals with DM (*44*, *45*), we analyzed the correlation between CCR2 abundance and SFTSV infection severity with respect to age and preexisting conditions. Through ex vivo infection, peripheral blood primary human monocytes isolated from both elderly individuals (≥60 years old) and individuals with DM were more susceptible to SFTSV binding than those prepared from individuals aged under 60 years and non-DM individuals, respectively (Fig. 6, A and B). On the basis of data from monocytes isolated from healthy donors of various ages, we confirmed a significantly positive correlation between the cell surface expression level of CCR2 and the binding ability of SFTSV ($R^2 = 0.735$, $P = 0.001$; Fig. 6C). A clinical investigation of 45 patients with SFTS further revealed a positive correlation between the CCR2 expression level on monocytes and the peak viral load in the serum samples that were consecutively collected during the clinical course ($R^2 = 0.76$, $P < 0.001$; Fig. 6D).

Plasmablasts were recently determined to be highly susceptible to SFTSV infection, with remarkable expansion in SFTS patients and correlated with lethal outcome (*31*, *46*). We simultaneously demonstrated increased expression levels of CCR2 on plasmablasts and plasma cells after their differentiation from B cells (fig. S11, A to C). Moreover, H929, a human myeloma plasma cell line with a high level of CCR2 expression, showed significantly higher susceptibility to SFTSV than other B cell lines (fig. S11, D and E). Together, these findings indicate that the higher expression level of CCR2 on monocytes and plasmablasts contributes to the poor disease prognosis and higher mortality observed in severe SFTS patients (*5*, *6*, *43*).

DISCUSSION

SFTSV has a broad host tropism that comprises humans, livestock, and wildlife and can infect a variety of cell types in patients such as epithelial cells, monocytes, and macrophages (*2*, *47*, *48*); thus, identification of host factors that mediate cell entry of SFTSV is important for understanding viral pathogenesis. Considering the broad spectrum of virus susceptible cells, it is conceivable that different receptors may mediate SFTSV infection of different cell types. Previous studies revealed that DC-SIGN can facilitate the entry of SFTSV (*24*, *25*), as well as other phenuiviruses such as RVFV and UUKV, in a glycosylation-dependent manner (*26*). Nonmuscle myosin heavy chain IIA (NMMHC IIA) was reported as an attachment factor for SFTSV infection, which contributes to SFTSV infection via endocytosis and phagocytosis (*49*). Despite these findings, the identification of a receptor that mediates SFTSV infection of key target cell types remains an unsolved endeavor.

Here, we performed a genome-wide CRISPR-Cas9–based screen and identified protocadherin 9 (PCDH9) and CCR2 as the top two hit genes. A close relative member of PCDH9, the cadherin-superfamily PCDH1, has been recognized as a critical host factor for cell entry by two bunyavirus members, Andes virus (ANDV) and Sin Nombre virus (SNV) (*50*), while knockdown of PCDH9 did not affect SFTSV, HRTV, or Guertu virus (GTV) binding to cells or infection at 4 hours after infection, suggesting that PCDH9 is not involved in the entry phase of SFTSV, HRTV, or GTV (fig. S12). The result that PCDH9 depletion reduced SFTSV replication at 24 hours after infection suggests that PCDH9 may regulate SFTSV infection events downstream of entry. Notably, depletion of CCR2 led to strongly reduced SFTSV binding and infection in both the human

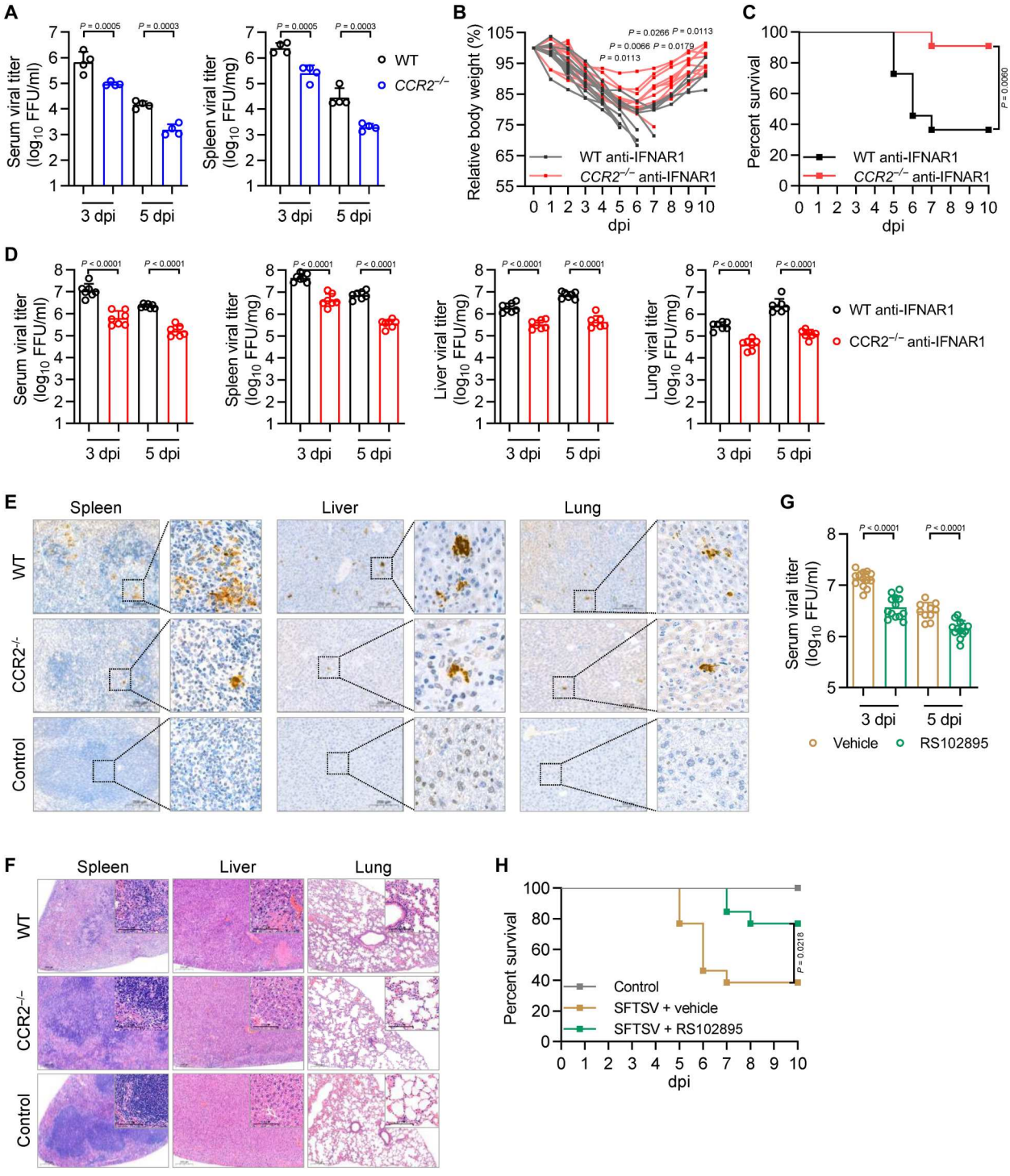

Fig. 5. CCR2 contributes to SFTSV pathogenesis in mouse models. (**A**) Serum and spleen viral titers in SFTSV-infected *CCR2*$^{-/-}$ and WT C57BL/6J mice (four for each group) tested by immunological focus assay at 3 and 5 dpi. (**B** and **C**) Survival probability (B) and relative body weight (C) in anti-IFNAR1 antibody–pretreated *CCR2*$^{-/-}$ (n = 11) and WT (n = 11) C57BL/6J mice after intraperitoneal infection with SFTSV. (**D**) Viral titers in serum, spleen, liver, and lung samples from anti-IFNAR1 antibody–pretreated *CCR2*$^{-/-}$ and WT C57BL/6J mice (four for each group) tested by immunological focus assay at 3 and 5 dpi. (**E** and **F**) Representative images of spleen, liver, and lung sections collected at 5 dpi from control and SFTSV-challenged *CCR2*$^{-/-}$ and WT C57BL/6J mice stained with a rabbit polyclonal antibody against SFTSV NP (E) or with hematoxylin and eosin (F). (**G**) Viral titers in serum from anti-IFNAR1 antibody–pretreated C57BL/6J mice tested by immunological focus assay at 3 (n = 13 for each group) and 5 (n = 10 for nontreated group and n = 13 for treated group) dpi. (**H**) Survival probability in anti-IFNAR1 antibody–pretreated C57BL/6J mice with SFTSV infection in the absence (n = 13) or presence (n = 13) of CCR2 antagonist RS102895 and without SFTSV infection (n = 5). Two-tailed Student's t test was performed for comparison of variables between two groups [(A), (B), (D), and (G)]. The Kaplan-Meier method was used to analyze time-to-event data [(C) and (H)].

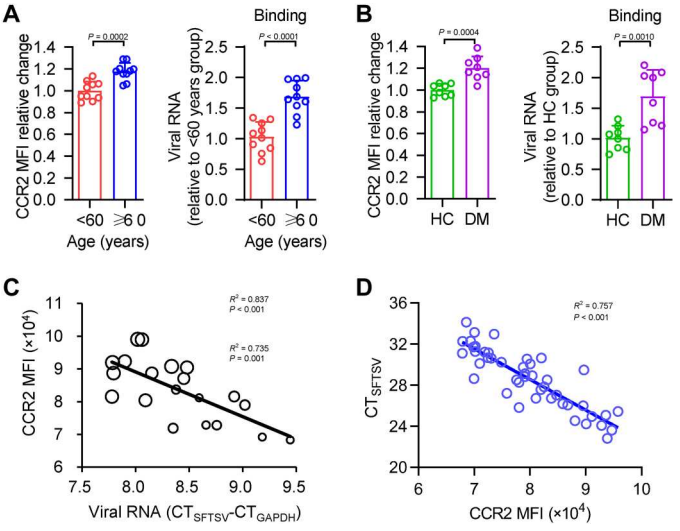

Fig. 6. CCR2 contributes to SFTSV infectivity in primary human monocytes. (**A** and **B**) Comparisons of surface CCR2 expression levels on primary human monocytes (left) and the ability of SFTS binding (right) between donors aged <60 (n = 10) and ≥60 (n = 10) years old (A), as well as between healthy donors (n = 8) and donors with DM (n = 8) (B). MFI, mean fluorescent intensity. (**C**) Association of surface CCR2 expression level on primary human monocytes with virus binding ability or with the age of donors (n = 20). R_a^2 indicates the correlation between the CCR2 expression level and individual age, and R_b^2 indicates the correlation between the CCR2 expression level and the binding ability of SFTSV. (**D**) Association of surface CCR2 expression level on primary human monocytes with the peak viral load in serum that was consecutively collected from SFTS patients (n = 45) during the clinical course. Two-tailed Student's t test was performed for comparison of variables between two groups [(A) and (B)]. R^2 [(C) and (D)] was estimated by a linear regression model. HC, healthy control; DM, diabetes mellitus; CT, cycle threshold.

monocytic THP-1 cell line and mouse primary BMDMs. The role of CCR2 in mediating virus binding appears specific to SFTSV because CCR2 depletion or CCR2 inhibitor treatment did not affect the binding of other bunyaviruses such as HRTV, RVFV, and AMRV. Of these viruses, HRTV is closely related to SFTSV; however, the anti-SFTSV Gn antibodies, Mab4-5 and Ab10, showed no cross-reaction with HRTV (*51*).

CCR2 has two isoforms, CCR2A and CCR2B, which have a common N-terminal extracellular domain that mediates direct binding with SFTSV Gn. We further showed that tyrosine sulfation at the Y26 site of the CCR2 N-terminal domain is critical for binding. This allowed the development of an inhibitory peptide derived from the CCR2 N-terminal region that significantly inhibited SFTSV binding and infection. A CCR2 antagonist exhibited significant protection against SFTSV infection in a lethal mouse infection model, further supporting its potential as a target for developing effective anti-SFTSV therapeutic measures.

CCR2 is highly expressed in monocytes and serves as a functional receptor for the chemokine CCL2 (*29*). We have demonstrated in our previous studies that monocytes are a major target cell type of SFTSV infection and trigger pathogenic inflammatory responses in SFTS patients (*31*, *42*). It is therefore possible that CCR2-mediated efficient SFTSV infection of monocytes may play important roles in promoting virus dissemination and inflammatory pathogenesis in patients. Whether additional receptors may mediate SFTSV infection of monocytes awaits further investigation.

Patients of older age or with underlying DM suffer a higher fatality rate from SFTSV infection (*5*, *6*, *43*), and the underlying reason is unclear. Here, we found that monocytes prepared from individuals of either older age or with DM showed a significantly up-regulated CCR2 expression level and supported more robust SFTSV infection. Considering the well-established functions of CCR2 in promoting inflammation, it can be speculated that CCR2-high monocytes could also trigger stronger inflammatory responses upon SFTSV infection. Together, these factors may lead to the worsened SFTS prognosis in elderly patients or those with underlying DM.

Recent studies have reported a robust differentiation process from naïve B cells into plasmablasts during the course of SFTSV infection in patients, with plasmablasts acting as a major target cell for SFTSV infection at the late stage of disease (*31*, *46*). Compared with naïve B cells, plasmablasts are more susceptible to SFTSV infection, leading to compromised antigen-presenting function and impaired humoral immune responses. We revealed significantly higher expression levels of CCR2 in both plasmablasts and the H929 B cell line than in other B cell types, which may explain their increased susceptibility to SFTSV infection. The higher expression level of CCR2 on monocytes and plasmablasts, two major target cell types of SFTSV in patients, further corroborates the critical role of CCR2 in mediating SFTSV infection and pathogenesis.

In summary, we established a critical role of CCR2 in mediating SFTSV entry in a variety of cell types and demonstrated the importance of CCR2 in SFTS disease pathogenesis based on mouse models and clinical data. Because SFTSV infects multiple organs in patients, it should also be noted that additional receptors may mediate SFTSV infection of other cell types and tissues. Nevertheless, considering the critical role of CCR2 in mediating SFTSV infection of monocytes and plasmablasts, two major target cell types that contribute to SFTS pathogenesis, it is worthwhile to develop therapeutic strategies targeting CCR2 in treating SFTSV infection.

MATERIALS AND METHODS

Study design

This study was designed to identify new host factors for cellular entry by SFTSV and to evaluate their potential efficiency as targets for developing anti-SFTSV therapeutic measures. We established an unbiased genome-wide CRISPR-Cas9–based screen to discover host factors for SFTSV entry and verified the role of hit genes in mediating viral binding and replication using virological and biochemical experiments. Gene KO mouse models were used to evaluate the effect of the hit gene on SFTSV infection and disease pathogenesis by virologic and histopathologic measurements. The effect of inhibitors or antibodies that block the interaction between SFTSV Gn and the entry factor was investigated in vitro and in mouse models. We also assessed the clinical relevance of the hit gene in the pathogenesis of SFTSV infection, especially its contribution to promoting viral infection and exacerbating poor prognosis. All experiments were conducted with the approval of the Institutional Animal Care and Use Committee at the Beijing Institute of Microbiology and Epidemiology (IACUC-IME-2021-003). The clinical sample collection was approved by the human ethics committee of the institute in accordance with the medical

research regulations of China (AF/SC-08/02.114). All participants provided written informed consent to have their samples and information collected.

Cells and viruses

THP-1, Jurkat, NALM-6, Raji, and BC-3 cells obtained from the American Type Culture Collection (ATCC), as well as H929 cells obtained from the China Center for Type Culture Collection (CCTCC), were maintained in RPMI 1640 medium (Gibco Invitrogen, catalog no. 11875093) containing 10% fetal bovine serum (FBS; Gibco Invitrogen, catalog no. 10099141) and 10 nM Hepes (Gibco Invitrogen, catalog no. 15630130). Raw264.7, Vero, and human embryonic kidney (HEK) 293T cells obtained from ATCC, Huh7 cells obtained from CCTCC, as well as HL-7702 cells obtained from Cell Bank of the Chinese Academy of Sciences (Shanghai, China) were maintained in Dulbecco′s modified Eagle′s medium (DMEM; Gibco Invitrogen, catalog no.11995065) containing 10% FBS and 10 mM Hepes. All the cells were cultured at 37°C in a humidified atmosphere of 5% CO_2.

For the preparation of BMDMs, femur and tibia bones were dissected from 6-week-old C57BL/6J mice, and bone marrow cells were collected under sterile conditions and then maintained in DMEM containing 10% FBS, 1% penicillin/streptomycin, and macrophage colony-stimulating factor (M-CSF; 50 ng/ml). After 7 days in culture, adherent cells were more than 90% pure BMDMs, which were used immediately for experiments or stored at −80°C.

SFTSV strain HBMC16_human_2015 (*52*), HRTV isolate patient 1 (*53*), and RVFV strain BJ01 (*54*) were obtained from the National Virus Resource Centre, and Amur virus (AMRV) (*55*) was obtained from the Beijing Institute of Microbiology and Epidemiology. The SFTSV strains WCH, HNXY2017-50, and HNXY2017-66 were isolated from serum samples of patients with SFTS in People′s Liberation Army 154 Hospital in Xinyang City of Henan Province, China. All viruses were propagated in Vero cells and used appropriately in this study. Experiments with viruses were performed in a biosafety level 2 (BSL-2; SFTSV) or 3 (BSL-3; HRTV, RVFV, and AMRV) facilities, in accordance with institutional biosafety operating procedures.

CRISPR-Cas9–based screen and data analysis

To construct the PB-CRISPR-human KO library, we synthesized DNA oligonucleotide library according to the genome-wide guide RNA list (*27*). The synthesized DNA oligonucleotides were amplified by polymerase chain reaction (PCR) using Q5 DNA polymerase (New England Biolabs) and purified using the QIAquick Gel Extraction Kit (Qiagen). The pCRISPR sg4 vector was digested with Bbs I (New England Biolabs), and the amplified sgRNA sequences were assembled into the vector backbone with the Gibson Assembly method. From the ligation, 20 μl of the ligation products was transformed into 100 μl of DH10B competent cells. To ensure no loss of representation, 10 individual electroporations were carried out and obtained approximately 10^7 recombinants, which yielded 80× library coverage (*28*). Bacteria were harvested, and the sgRNA library plasmids were extracted using the endotoxin-free plasmid Maxiprep (Qiagen). The PB-CRISPR-human KO library, pCRISPR S10, and PBase plasmids were simultaneously electrotransfected with 2×10^8 Huh7 cells (Lonza 2B). On the second day after transduction, the cell medium was changed to fresh medium containing puromycin (2 μg/ml). A total of 7×10^7 mixed library cells were obtained, and the genomes were extracted. The sgRNA sequences were amplified and subjected to the next-generation sequencing analysis to obtain cell mutation library with 100× coverage.

A total of 1×10^8 cell mutation libraries were inoculated with authentic SFTSV at an MOI of 5 and then incubated for 48 hours, which allowed nearly all cells to become infected. Next, cells that were negative for SFTSV infection were sorted by fluorescence-activated cell sorting using a mouse monoclonal antibody against SFTSV NP on a Calibur flow cytometer (BD Biosciences). Genomic DNA was extracted from uninfected cells (5×10^7) or SFTSV NP-negative sorted cells (1×10^7) by TIANGEN kits (TIANGEN BIOTECH). The concentration was examined using an ultraviolet-visible spectrophotometer (Quawell Technology). For each sample, the sgRNA-coding region was amplified by using Q5 Hot Start High-Fidelity DNA Polymerase (New England Biolabs). Ten micrograms of total genomic DNA was amplified with the following conditions: 95°C for 3 min, 32 cycles at 95°C for 30 s, 55°C for 30 s and 72°C for 30 s, 72°C for 5 min. Forty PCRs were performed.

The sgRNA sequences were amplified and subjected to next-generation sequencing using a HiSeq 2500 platform (Illumina). The raw data were removed from the PCR sequences using cutadapt software and then compared with the predefined target database using bowtie2 software to generate the comparison results. The program counts the number of reads for each sgRNA, counts the number of reads for sgRNAs, and calculates the *z* score. Two replicated experiments were performed, and the mean of the *z* score was calculated.

RNA interference knockdown

THP-1 and Raw264.7 cells preseeded in 24-well plates (10^5 cells per well) were transfected with small interfering RNAs (siRNAs) using Lipofectamine RNAiMAX (Invitrogen, catalog no. 13778150), according to the manufacturer′s instructions. In the parallel experiment, scramble siRNA was included as a control. Seventy-two hours after transfection, cells were inoculated with SFTSV or a negative control and collected for reverse transcription quantitative PCR (RT-qPCR), Western blot, or flow cytometry analysis at 24 hours after infection. All siRNA oligonucleotides used in the study were synthesized by GenePharma (Suzhou, China). The siRNA sequences are as follows: 5′-GGCTGTATCACATCGGTTA TT-3′ (#1) and 5′-GAGGAUGGAAUAAUUUCCATT-3′ (#2) for Huh7 and THP-1 cells and 5′-CUGUGUGAUUGACAAGCACT T-3′ (#1) and 5′- CCUCUCUACCAGGAAUCAUTT-3′ (#2) for Raw264.7 cells, respectively.

Construction of *CCR2*-KO THP-1 cells

The human *CCR2* gene sgRNA (sequence: 5′-GCAGCAGAGTGA GCCCACAA-3′) or the control sgRNA (sequence: 5′-GTATTACT GATATTGGTGGG-3′) without human genome target was cloned into lentiCRISPR v.2 (Addgene, catalog no. 52961) and packaged into HEK293T cells with pCMV-dR8.91 and pMD2.G (Addgene, catalog no. 12259) using Lipofectamine 2000 (Thermo Fisher Scientific, catalog no. 11668019). THP-1 cells were transduced with lentiviruses containing *CCR2* sgRNA or control sgRNA and selected for 7 days in the presence of puromycin. Clonal CCR2-deficient cell lines were obtained by limiting dilution and validated by flow cytometry analysis using an anti-CCR2 antibody (BioLegend,

catalog no. 357205) and Sanger sequencing method with the use of primers [5′-GAGCGGTGAAGAAGTCACCA-3′ (forward) and 5′-CAGAAGCAAACACAGCCACC-3′ (reverse)].

CCR2 overexpression in cells

The pLX304 plasmids encoding C-terminal V5-tagged human CCR2 isoform A and CCR2 isoform B were obtained from the CCSB-Broad Lentiviral Expression Library (Dharmacon). The deletion of 29 N-terminal amino acids and the Y26F site mutation in human CCR2 expression pLX304 plasmids were constructed by using the In-Fusion Cloning Kit (Taraka, catalog no. 639648) and verified by Sanger sequencing. Lentiviruses were produced as described above. Cells were transduced with lentiviruses and selected for 7 days in the presence of blasticidin S. The expression of CCR2 in cells was verified by flow cytometry or Western blot analysis.

RT-qPCR assay

Total RNA was extracted from cells per tissue and cell culture supernatant with the RNAprep Pure Cell Kit (TIANGEN, catalog no. DP430) and TIANamp Virus RNA Kit (TIANGEN, catalog no. DP315-R), respectively, according to the manufacturer′s instructions. Relative quantitation of intracellular vRNA was measured by using RT-qPCR based on the S segment of the respective virus. The primer sequences for vRNA quantification of SFTSV (*11*), HRTV (*33*), and RVFV (*54*) were obtained from previous studies.

Western blot analysis

Cells treated as indicated were lysed with lysis buffer. Lysates with Laemmli sample buffer (containing DL-dithiothreitol) were heated for 10 min at 56°C, subjected to 12 to 15% SDS-polyacrylamide gel electrophoresis, and then transferred to polyvinylidene difluoride membranes (Millipore, catalog no. IPVH00010). Proteins were further incubated with the indicated primary antibodies and then with horseradish peroxidase–conjugated secondary antibodies. Protein bands were detected by an enhanced chemiluminescence kit (Millipore, catalog no. WBKLS0500) using a chemiluminescence analyzer (Bio-Rad).

Immunological focus assay

Vero cell monolayers were infected with SFTSV (MOI = 1) and incubated under a methylcellulose overlay. At 48 hours after infection, Vero cell monolayers were fixed with 4% formaldehyde in phosphate-buffered saline (PBS) and permeabilized by incubation with 0.5% Triton X-100 in the balanced salt solution. The cells were then stained with a mouse monoclonal antibody against SFTSV NP and horseradish peroxidase–labeled secondary antibody (Applygen, catalog no. C1308-3).

Indirect immunofluorescence assay

Cells grown on glass coverslips were fixed with 4% paraformaldehyde for 30 min at room temperature and then washed twice with PBS. The cells were stained with wheat germ agglutinin (WGA) fluorescein conjugate (Invitrogen, catalog no. W834), which was diluted 1:100 with Hanks′ balanced salt mixture (Solarbio, catalog no. H1025) for 10 min, washed with PBS, and subsequently stained with a mouse monoclonal antibody against SFTSV NP as a primary antibody diluted 1:1000 with 5% bovine serum albumin (BSA) and 1% Triton X-100 (to permeabilize and block cells) for 4 hours. Alexa Fluor 568 goat anti-mouse IgG (H+L) secondary antibody (Invitrogen, catalog no. A11004) was used at a dilution of 1: 1000 for 1 hour. After washing three times with PBS, cell nuclei were stained with 4′,6-diamidino-2-phenylindole (DAPI). Immunofluorescence images were acquired using the Cytation 1 Cell Imaging Multi-Mode Reader (BioTek).

Flow cytometry analysis

For intracellular virus detection, cells were fixed with the commercial Cytofix/Cytoperm Fixation/Permeabilization Solution Kit (BD Biosciences, catalog no. 554714) according to the manufacturer′s instructions. Then, the cells were stained with a mouse monoclonal antibody against SFTSV NP (diluted 1:1000) overnight at 4°C. Antibodies bound to cells were detected using fluorescein-5-isothiocyanate–conjugated goat anti-mouse IgG (TransGen Biotech, catalog no. HS211-01). For detection of surface CCR2 expression, different cell lines or cells that were transduced with recombinant lentivirus expressing CCR2A, CCR2B, CCR2A/B-N14Q, CCR2A/B-Y26F, or CCR2A/B-ΔN for 72 hours were washed with PBS, blocked with human Fc block (diluted 1:100; BD Biosciences) for 10 min at room temperature to avoid nonspecific binding, and then stained for CCR2 with allophycocyanin (APC)/Cyanine 7 anti-human CD192 (CCR2) (BioLegend, catalog no. 357220) or phycoerythrin (PE) anti-human CD192 (CCR2) (BioLegend, catalog no. 357205) for 30 min at 4°C. All flow cytometry experiments were carried out using the Novocyte 3310 System (ACEC Biosciences). Samples were analyzed using NovoExpress software (ACEC Biosciences) or FlowJo software version 10.2 (Tree Star Inc.).

SFTSV internalization and binding assays

For the virus internalization assay, SFTSV virions (MOI = 10) were incubated with cells at 4°C for 1 hour. After washing three times with precooled PBS and 2% BSA, prewarmed 37°C medium containing 2% FBS and ammonium chloride was added to the cells, and the cells were subsequently incubated at 37°C for 3 hours to allow virus internalization. The cells were then washed with PBS and treated with trypsin to remove bound virions. The internalized virions were measured with RT-qPCR. For the virus binding assay, SFTSV virions (MOI = 10) were incubated with cells at 4°C for 1 hour. After washing three times with precooled PBS, the relative level of bound viral particles was quantified via RT-qPCR. For the binding assay with microscopy, BMDMs and THP-1 cells were infected with SFTSV at an MOI of 50 in the presence of ammonium chloride for 1 hour. After washing three times with precooled PBS and brief treatment with trypsin, cells were fixed with 4% paraformaldehyde and labeled with a mouse monoclonal antibody against SFTSV NP and goat anti-mouse fluorescent secondary antibody for microscopy analysis.

CCR2 antagonist and anti-human CCR2 antibody inhibition assays

THP-1 and Huh7 cells were pretreated with serial concentrations of two CCR2 antagonists, CCR2 antagonist RS102895 hydrochloride (MedChemExpress, catalog no. 1173022-16-6) and CCR2 antagonist 1 (MedChemExpress, catalog no. 1683534-96-4), and an anti-human CCR2 antibody (BioLegend, catalog no. 357202) or IgG isotype control (BioLegend, catalog no. 400201). After 1 hour, the cells were infected with SFTSV at an MOI of 1 or 5. At 24 hours after infection, the cells were harvested and subjected to measurement of

intracellular vRNA levels by using RT-qPCR, Western blot, or flow cytometry analysis using a rabbit polyclonal antibody against SFTSV NP, and the supernatant was collected for examination of viral titers.

Peptide inhibition assays

Peptides p1 (EEVTTFFDYDYGAP) and p2 (EEVTTFFDY[SO_3]DYGAP) and a scrambled control peptide (EDFVYPDFATEYTG) were synthesized with 95% purity by Bankpeptide (Hefei, China). SFTSV was incubated with serial dilutions of each peptide for 2 hours at 37°C and then inoculated on THP-1 cells. Intracellular vRNA levels 24 hours after infection and bound virion levels in the virus binding assay were measured with RT-qPCR as described above.

Coimmunoprecipitation of CCR2A and CCR2B

The pCAGGS-SFSTV-Gn-strep plasmid and the C-terminal Flag-tagged CCR2 isoform A, isoform B, SCARB1, GFP, or vector pCDH-CMV-MCS-EF1-Flag plasmids were cotransfected into HEK293T cells for 48 hours and lysed in lysis buffer [150 mM NaCl, 100 mM tris-HCl (pH 8.0), 1% lauryl maltose neopentyl glycol (LMNG; Anatrace), and 0.2% cholesteryl hemisuccinate tris salt (CHS; Anatrace) containing EDTA-free protease inhibitor cocktails (Roche)]. After removal of cell debris by centrifugation, $^1/_{10}$th of the volume of lysates was used as whole-cell lysate input. For Strep-IP, half of the lysates were bound to MagStrep XT beads (IBA, catalog no. 2-4090-002) for 2 hours at 4°C. For Flag-IP, the remaining half of the lysates were bound to anti-Flag M2 beads (Sigma-Aldrich, catalog no. M8823). The beads were washed once with 1 ml of Wash Buffer I [150 mM NaCl, 100 mM tris-HCl (pH 8.0), 0.5% LMNG, and 0.04% CHS] and twice with 1 ml of Wash Buffer II [150 mM NaCl, 100 mM tris-HCl (pH 8.0), 0.001% LMNG, 0.04% CHS, and 0.1% n-Dodecyl-β-D-Maltopyranoside (DDM)] and analyzed by Western blotting.

Biotinylation of cell surface proteins

HEK293T cells overexpressing the indicated proteins were chilled on ice for 10 min and labeled with 2 mM biotin (Thermo Fisher Scientific, catalog no. 21338) in PBS for 30 min on ice. The unbound biotin was quenched with 100 mM glycine in PBS for 5 min, which was repeated three times. After washing with PBS, cells were lysed in lysis buffer and immunoprecipitated with streptavidin beads (GenScript, catalog no. L00424) or protein G beads (Bio-Rad, catalog no. 1614833) bound to rabbit anti-V5 antibody for 2 hours at 4°C. The beads were then washed once with Wash Buffer I and twice with Wash Buffer II and analyzed by Western blotting.

Assay of peptide binding to virus

To quantify peptides that can bind SFTSV virions, the virus-containing culture supernatants were purified to a titer of approximately 10^9 plaque-forming units/ml with the use of Ultra 15 Centrifugal Filter Devices (Amicon). The Mab4-5 antibody (*21*) and purified SFTSV viruses were coincubated with protein G beads for 1 hour at 4°C, followed by washing three times using PBS-T (0.1% Tween-20). The beads were then incubated with 20 mM peptides in PBS for 1 hour at 4°C, followed by washing three times with PBS-T and three times with PBS. Gn protein bound to beads was detected by Western blot. Peptides bound to beads were then purified, and the absolute quantity of each peptide that was coimmunoprecipitated with SFTSV was determined by using a PRM assay, a targeted MS method.

PRM assay

For peptide detection, the eluates from beads were filtered by 10 kDa centrifugal filters (Merck Millipore). The flow-throughs were collected and subjected to C18 columns for peptide desalting and purification. The obtained peptide samples were analyzed on a Q Exactive Plus mass spectrometer coupled with an EASY-nLC 1200 liquid chromatography (LC) system. LC-MS/MS data acquisition was performed in PRM mode. Briefly, data were acquired using a spray voltage of 2.2 kV and ion transfer tube temperature of 320°C. Each scan cycle consisted of one full MS1 scan mass spectrum [resolution, 70,000; scan range, 6002; 400 mass/charge ratio, automatic gain control (AGC), 3×10^6; injection time (IT), 50 ms], followed by target MS/MS scans (resolution, 17,500; AGC, 2×10^5; IT, 100 ms). The isolation window was set to 1.2 Da. The higher-energy collisional dissociation was set to 28.. PRM MS raw files were analyzed using Skyline software for extracted ion chromatogram (XIC) generation, peak integration, and quantification of the target peptides. All peaks were inspected manually to ensure the correct detection of precursor and fragment ions. The summed peak area of the most intense fragment ions was used to quantify the target peptides. A standard curve was built from synthetic peptides with diluted concentrations using the same PRM method.

SFTSV infectivity in different B cell lines

Raji, BC-3, NALM-6, and H929 cells were inoculated with SFTSV strain HBMC16 at an MOI of 5 and then incubated for 24 hours. SFTSV infection rates in the cells were tested by flow cytometry with a mouse monoclonal antibody against SFTSV NP. The cell surface expression level on these cells was tested by flow cytometry with APC/Cyanine 7 anti-human CD192.

CCR2 expression level in B cell subtypes

Our previously reported 10x Genomics single-cell RNA-sequencing data from 27 peripheral blood mononuclear cell (PBMC) samples were reanalyzed (*31*). Eight subtypes of B cells were determined. Uniform manifold approximation and projection analysis of CCR2 was performed in the eight B cell types. A dot plot showing the CCR2 gene across B cell subtypes was constructed by using the Seurat Dotplot function.

Mouse experiments

C57BL/6J mice deficient in CCR2 (CCR2$^{-/-}$; B6.129S4-*Ccr2*^{tm1Ifc}/J) were obtained from The Jackson Laboratory. The deletion of CCR2 was verified by PCR assay using the following primers: CCR2-Co-F3, 5′-TGCTCACCAGGAAATGCCAGG-3′; CCR2-Mu-R3, 5′-CTGAGGCGGAAAGAACCAGC-3′; and CCR2-Wt-R3, 5′-TGAGCAGGAAGAGCAGGTCAGAG-3′. The mice were kept in an environmentally controlled specific pathogen–free animal facility in the State Key Laboratory of Pathogens and Biosecurity (Beijing, China). Five-week-old female CCR2$^{-/-}$ and WT C57BL/6J mice were intraperitoneally inoculated with 100 μl of virus solution [2×10^5 focus-forming units (FFU)/ml]. Four mice from each group were sacrificed at 3 and 5 dpi, and spleen samples were collected for detection of virus titers. A lethal mouse model was also established by using an anti–interferon α/β receptor subunit 1 (IFNAR1)

blocking antibody (Bio X Cell, catalog no. BE0241) pretreatment to evaluate the pathogenesis of SFTSV infection (*33*). Briefly, 5-week-old female CCR2$^{-/-}$ (n = 11) and WT (n = 11) C57BL/6J mice were treated with anti-IFNAR1 IgG (1.7 mg per mouse) by intraperitoneal injection 1 day before infection. Mice were intraperitoneally inoculated with 100 μl of virus solution (2×10^4 FFU/ml) at day 0. The body weight and survival rate of the mice were monitored each day. After dissection of CCR2$^{-/-}$ and WT C57BL/6J mice 3 and 5 dpi, serum samples were collected for detection of virus titers (four mice for each group), and spleen and liver samples were collected for examination of virus titers and histopathology (hematoxylin and eosin staining). Viral titers were determined by immunological focus assays or immunohistochemistry using a mouse monoclonal antibody against SFTSV NP. The treatment effect of the CCR2 antagonist RS102895 was investigated in anti-IFNAR1 antibody–pretreated C57BL/6J mice that were inoculated with 100 μl of virus solution (2×10^4 FFU/ml), with 5 mice for the control group, 13 for the SFTSV + vehicle group, and 13 for the SFTSV + RS102895 group. The CCR2 antagonist RS102895 was dissolved in 20% sulfobutylether- β-cyclodextrin (SBE-β-CD) in saline and administered by a stomach probe at a dose of 15 mg/kg per day. Approximately 50 μl of caudal vein blood samples was collected for serum separation at 3 and 5 dpi, and the viral titer in serum was quantified as mentioned above. Spleen and liver samples were collected at 5 dpi for histopathology and immunohistochemistry analysis. In vivo studies were not blinded, and mice were randomly assigned to each treatment group.

Ex vivo infection of primary monocytes from healthy donors

PBMCs were isolated from healthy donors via density gradient centrifugation using Ficoll-Paque Plus medium (GE Healthcare) and washed with Ca/Mg-free PBS. The PBMC fraction was then treated with red blood cell lysis buffer (BioLegend) to remove red blood cells and washed with Ca/Mg-free PBS containing 2% FBS. Isolated PBMCs were then subjected to the purification of monocytes by using the Pan-monocyte Isolation Kit (Miltenyi), according to the manufacturer's instructions. Briefly, PBMCs were blocked with 10 μl of Fc receptor–blocking reagent, stained with 10 μl of biotin-antibody cocktail for 10 min at 4°C, and subsequently stained with 20 μl of antibiotin microbeads (Miltenyi) for 15 min at 4°C. Then, PBMC suspension was infused through an LS cell separation column (Miltenyi) placed in the MACS Separator (Miltenyi), and the negative fraction containing enriched and unlabeled monocytes was collected and counted. The purity of the isolated monocyte populations was determined by flow cytometry using the markers CD45, CD14, and CD16 and was found to be >95% pure. The surface expression of CCR2 on purified monocytes was examined by flow cytometry analysis. Monocytes were infected with SFTSV at an MOI of 10 for the virus binding assay as mentioned above.

Clinical investigation of the association between monocyte CCR2 expression level and viral load in patients with SFTS

We conducted a clinical study on patients with SFTS at the People's Liberation Army 990 Hospital, the local designated hospital for treating SFTS (*5*). During the follow-up period from 1 July to 31 August 2021, we collected whole-blood samples from 45 surviving SFTS patients who had been hospitalized for at least 5 days. PBMCs were isolated, and then the monocytes were purified. The cell surface CCR2 expression level of the monocytes was examined by flow cytometry analysis. Serial samples collected during hospitalization from the 45 patients were used for quantification of SFTSV RNA levels. The mean (SD) age of the patients was 62.9 (9.8), and 55.6% were female. The association between the highest level of serum viral load and the CCR2 expression level of monocytes was analyzed.

Statistical analysis

All values or percentages were from at least three biological replicates. Continuous variables were summarized as the means and SDs. Student's t test was used for comparisons of continuous variables between two groups, and one-way analysis of variance (ANOVA) followed by Tukey's multiple comparisons test was used for comparisons of continuous variables among multiple groups. R^2 was estimated for dose-dependent analysis by using nonlinear regression model. We used the Kaplan-Meier method and the log-rank test to analyze time-to-event data for treatment effect analysis. A two-sided P value of <0.05 was considered statistically significant. All statistical analyses were performed using SPSS software, version 19.0.

Supplementary Materials

This PDF file includes:

Figs. S1 to S12
Table S1

REFERENCES AND NOTES

1. V. S. Balakrishnan, WHO launches global initiative for arboviral diseases. *Lancet Microbe* **3**, e407 (2022).
2. X. J. Yu, M. F. Liang, S. Y. Zhang, Y. Liu, J. D. Li, Y. L. Sun, L. Zhang, Q. F. Zhang, V. L. Popov, C. Li, J. Qu, Q. Li, Y. P. Zhang, R. Hai, W. Wu, Q. Wang, F. X. Zhan, X. J. Wang, B. Kan, S. W. Wang, K. L. Wan, H. Q. Jing, J. X. Lu, W. W. Yin, H. Zhou, X. H. Guan, J. F. Liu, Z. Q. Bi, G. H. Liu, J. Ren, H. Wang, Z. Zhao, J. D. Song, J. R. He, T. Wan, J. S. Zhang, X. P. Fu, L. N. Sun, X. P. Dong, Z. J. Feng, W. Z. Yang, T. Hong, Y. Zhang, D. H. Walker, Y. Wang, D. X. Li, Fever with thrombocytopenia associated with a novel bunyavirus in China. *N. Engl. J. Med.* **364**, 1523–1532 (2011).
3. Y. R. Kim, Y. Yun, S. G. Bae, D. Park, S. Kim, J. M. Lee, N. H. Cho, Y. S. Kim, K. H. Lee, Severe fever with thrombocytopenia syndrome virus infection, South Korea, 2010. *Emerg. Infect. Dis.* **24**, 2103–2105 (2018).
4. T. Takahashi, K. Maeda, T. Suzuki, A. Ishido, T. Shigeoka, T. Tominaga, T. Kamei, M. Honda, D. Ninomiya, T. Sakai, T. Senba, S. Kaneyuki, S. Sakaguchi, A. Satoh, T. Hosokawa, Y. Kawabe, S. Kurihara, K. Izumikawa, S. Kohno, T. Azuma, K. Suemori, M. Yasukawa, T. Mizutani, T. Omatsu, Y. Katayama, M. Miyahara, M. Ijuin, K. Doi, M. Okuda, K. Umeki, T. Saito, K. Fukushima, K. Nakajima, T. Yoshikawa, H. Tani, S. Fukushi, A. Fukuma, M. Ogata, M. Shimojima, N. Nakajima, N. Nagata, H. Katano, H. Fukumoto, Y. Sato, H. Hasegawa, T. Yamagishi, K. Oishi, I. Kurane, S. Morikawa, M. Saijo, The first identification and retrospective study of severe fever with thrombocytopenia syndrome in Japan. *J. Infect. Dis.* **209**, 816–827 (2014).
5. H. Li, Q. B. Lu, B. Xing, S. F. Zhang, K. Liu, J. Du, X. K. Li, N. Cui, Z. D. Yang, L. Y. Wang, J. G. Hu, W. C. Cao, W. Liu, Epidemiological and clinical features of laboratory-diagnosed severe fever with thrombocytopenia syndrome in China, 2011–17: A prospective observational study. *Lancet Infect. Dis.* **18**, 1127–1137 (2018).
6. J. C. Li, Y. N. Wang, J. Zhao, H. Li, W. Liu, A review on the epidemiology of severe fever with thrombocytopenia syndrome. *Zhonghua Liu Xing Bing Xue Za Zhi* **42**, 2226–2233 (2021).
7. X. C. Tran, Y. Yun, L. Van An, S. H. Kim, N. T. P. Thao, P. K. C. Man, J. R. Yoo, S. T. Heo, N. H. Cho, K. H. Lee, Endemic severe fever with thrombocytopenia syndrome, Vietnam. *Emerg. Infect. Dis.* **25**, 1029–1031 (2019).
8. A. Zohaib, J. Zhang, M. Saqib, M. A. Athar, M. H. Hussain, J. Chen, A. U. Sial, M. H. Tayyab, M. Batool, S. Khan, Y. Luo, C. Waruhiu, Z. Taj, Z. Hayder, R. Ahmed, A. B. Siddique, X. Yang, M. A. Qureshi, I. U. Ujjan, A. Lail, I. Khan, R. Sajjad Ur, T. Zhang, F. Deng, Z. Shi, S. Shen,

Serologic evidence of severe fever with thrombocytopenia syndrome virus and related viruses in Pakistan. *Emerg. Infect. Dis.* **26**, 1513–1516 (2020).
9. A. M. Win, Y. T. H. Nguyen, Y. Kim, N. Y. Ha, J. G. Kang, H. Kim, B. San, O. Kyaw, W. W. Htike, D. O. Choi, K. H. Lee, N. H. Cho, Genotypic heterogeneity of Orientia tsutsugamushi in scrub typhus patients and thrombocytopenia syndrome co-infection, Myanmar. *Emerg. Infect. Dis.* **26**, 1878–1881 (2020).
10. M. D. S. Ongkittikul, M. D. R. Watanawong, R. N. P. Rompho, Severe fever with thrombocytopenia syndrome virus: The first case report in Thailand. *BKK Med. J.* **16**, 204–206 (2020).
11. L. Zhuang, Y. Sun, X. M. Cui, F. Tang, J. G. Hu, L. Y. Wang, N. Cui, Z. D. Yang, D. D. Huang, X. A. Zhang, W. Liu, W. C. Cao, Transmission of severe fever with thrombocytopenia syndrome virus by *Haemaphysalis longicornis* ticks, China. *Emerg. Infect. Dis.* **24**, 868–871 (2018).
12. A. C. G. Heath, A history of the introduction, establishment, dispersal and management of *Haemaphysalis longicornis* Neumann, 1901 (Ixodida: Ixodidae) in New Zealand. *N. Z. J. Zool.* **47**, 241–271 (2020).
13. D. Miao, K. Dai, G. P. Zhao, X. L. Li, W. Q. Shi, J. S. Zhang, Y. Yang, W. Liu, L. Q. Fang, Mapping the global potential transmission hotspots for severe fever with thrombocytopenia syndrome by machine learning methods. *Emerg. Microbes Infect.* **9**, 817–826 (2020).
14. X. Fang, J. Hu, Z. Peng, Q. Dai, W. Liu, S. Liang, Z. Li, N. Zhang, C. Bao, Epidemiological and clinical characteristics of severe fever with thrombocytopenia syndrome bunyavirus human-to-human transmission. *PLOS Negl. Trop. Dis.* **15**, e0009037 (2021).
15. World Health Organization, "Annual review of diseases prioritized under the Research and Development Blueprint" (WHO Meeting Report, 2017).
16. KCDC, KCDC Infectious Disease Portal Web Site (2020).
17. NIID, Severe fever with thrombocytopenia syndrome (SFTS) in Japan, as of June 2019. *IASR* **40**, 111–112 (2019).
18. X. J. Yu, Risk factors for death in severe fever with thrombocytopenia syndrome. *Lancet Infect. Dis.* **18**, 1056–1057 (2018).
19. M. Dessau, Y. Modis, Crystal structure of glycoprotein C from Rift Valley fever virus. *Proc. Natl. Acad. Sci. U.S.A.* **110**, 1696–1701 (2013).
20. S. S. Ganaie, M. M. Schwarz, C. M. McMillen, D. A. Price, A. X. Feng, J. R. Albe, W. Wang, S. Miersch, A. Orvedahl, A. R. Cole, M. F. Sentmanat, N. Mishra, D. A. Boyles, Z. T. Koenig, M. R. Kujawa, M. A. Demers, R. M. Hoehl, A. B. Moyle, N. D. Wagner, S. H. Stubbs, L. Cardarelli, J. Teyra, A. McElroy, M. L. Gross, S. P. J. Whelan, J. Doench, X. Cui, T. J. Brett, S. S. Sidhu, H. W. Virgin, T. Egawa, D. W. Leung, G. K. Amarasinghe, A. L. Hartman, Lrp1 is a host entry factor for Rift Valley fever virus. *Cell* **184**, 5163–5178.e24 (2021).
21. Y. Wu, Y. Zhu, F. Gao, Y. Jiao, B. O. Oladejo, Y. Chai, Y. Bi, S. Lu, M. Dong, C. Zhang, G. Huang, G. Wong, N. Li, Y. Zhang, Y. Li, W. H. Feng, Y. Shi, M. Liang, R. Zhang, J. Qi, G. F. Gao, Structures of phlebovirus glycoprotein Gn and identification of a neutralizing antibody epitope. *Proc. Natl. Acad. Sci. U.S.A.* **114**, E7564–E7573 (2017).
22. M. Spiegel, T. Plegge, S. Pohlmann, The role of phlebovirus glycoproteins in viral entry, assembly and release. *Viruses* **8**, 202 (2016).
23. S. M. de Boer, J. Kortekaas, C. A. de Haan, P. J. Rottier, R. J. Moormann, B. J. Bosch, Heparan sulfate facilitates Rift Valley fever virus entry into the cell. *J. Virol.* **86**, 13767–13771 (2012).
24. H. Tani, M. Shimojima, S. Fukushi, T. Yoshikawa, A. Fukuma, S. Taniguchi, S. Morikawa, M. Saijo, Characterization of glycoprotein-mediated entry of severe fever with thrombocytopenia syndrome virus. *J. Virol.* **90**, 5292–5301 (2016).
25. H. Hofmann, X. Li, X. Zhang, W. Liu, A. Kuhl, F. Kaup, S. S. Soldan, F. Gonzalez-Scarano, F. Weber, Y. He, S. Pohlmann, Severe fever with thrombocytopenia virus glycoproteins are targeted by neutralizing antibodies and can use DC-SIGN as a receptor for pH-dependent entry into human and animal cell lines. *J. Virol.* **87**, 4384–4394 (2013).
26. P. Y. Lozach, A. Kuhbacher, R. Meier, R. Mancini, D. Bitto, M. Bouloy, A. Helenius, DC-SIGN as a receptor for phleboviruses. *Cell Host Microbe* **10**, 75–88 (2011).
27. O. Shalem, N. E. Sanjana, E. Hartenian, X. Shi, D. A. Scott, T. Mikkelson, D. Heckl, B. L. Ebert, D. E. Root, J. G. Doench, F. Zhang, Genome-scale CRISPR-Cas9 knockout screening in human cells. *Science* **343**, 84–87 (2014).
28. C. Xu, X. Qi, X. Du, H. Zou, F. Gao, T. Feng, H. Lu, S. Li, X. An, L. Zhang, Y. Wu, Y. Liu, N. Li, M. R. Capecchi, S. Wu, piggyBac mediates efficient in vivo CRISPR library screening for tumorigenesis in mice. *Proc. Natl. Acad. Sci. U.S.A.* **114**, 722–727 (2017).
29. I. F. Charo, S. J. Myers, A. Herman, C. Franci, A. J. Connolly, S. R. Coughlin, Molecular cloning and functional expression of two monocyte chemoattractant protein 1 receptors reveals alternative splicing of the carboxyl-terminal tails. *Proc. Natl. Acad. Sci. U.S.A.* **91**, 2752–2756 (1994).
30. L. K. Zhang, B. Wang, Q. Xin, W. Shang, S. Shen, G. Xiao, F. Deng, H. Wang, Z. Hu, M. Wang, Quantitative proteomic analysis reveals unfolded-protein response involved in severe fever with thrombocytopenia syndrome virus infection. *J. Virol.* **93**, e00308-19 (2019).
31. H. Li, X. Li, S. Lv, X. Peng, N. Cui, T. Yang, Z. Yang, C. Yuan, Y. Yuan, J. Yao, Z. Yuan, J. Li, X. Ye, X. Zhang, S. Zhu, K. Peng, W. Liu, Single-cell landscape of peripheral immune responses to fatal SFTS. *Cell Rep.* **37**, 110039 (2021).
32. C. Jin, M. Liang, J. Ning, W. Gu, H. Jiang, W. Wu, F. Zhang, C. Li, Q. Zhang, H. Zhu, T. Chen, Y. Han, W. Zhang, S. Zhang, Q. Wang, L. Sun, Q. Liu, J. Li, T. Wang, Q. Wei, S. Wang, Y. Deng, C. Qin, D. Li, Pathogenesis of emerging severe fever with thrombocytopenia syndrome virus in C57/BL6 mouse model. *Proc. Natl. Acad. Sci. U.S.A.* **109**, 10053–10058 (2012).
33. H. Li, L. K. Zhang, S. F. Li, S. F. Zhang, W. W. Wan, Y. L. Zhang, Q. L. Xin, K. Dai, Y. Y. Hu, Z. B. Wang, X. T. Zhu, Y. J. Fang, N. Cui, P. H. Zhang, C. Yuan, Q. B. Lu, J. Y. Bai, F. Deng, G. F. Xiao, W. Liu, K. Peng, Calcium channel blockers reduce severe fever with thrombocytopenia syndrome virus (SFTSV) related fatality. *Cell Res.* **29**, 739–753 (2019).
34. Z. N. Dai, X. F. Peng, J. C. Li, J. Zhao, Y. X. Wu, X. Yang, T. Yang, S. F. Zhang, K. Dai, X. G. Guan, C. Yuan, Z. D. Yang, N. Cui, Q. B. Lu, Y. Huang, H. Fan, X. A. Zhang, G. F. Xiao, K. Peng, L. K. Zhang, W. Liu, H. Li, Effect of genomic variations in severe fever with thrombocytopenia syndrome virus on the disease lethality. *Emerg. Microbes Infect.* **11**, 1672–1682 (2022).
35. L. M. Wong, S. J. Myers, C. L. Tsou, J. Gosling, H. Arai, I. F. Charo, Organization and differential expression of the human monocyte chemoattractant protein 1 receptor gene. Evidence for the role of the carboxyl-terminal tail in receptor trafficking. *J. Biol. Chem.* **272**, 1038–1045 (1997).
36. J. Rucker, M. Samson, B. J. Doranz, F. Libert, J. F. Berson, Y. Yi, R. J. Smyth, R. G. Collman, C. C. Broder, G. Vassart, R. W. Doms, M. Parmentier, Regions in β-chemokine receptors CCR5 and CCR2b that determine HIV-1 cofactor specificity. *Cell* **87**, 437–446 (1996).
37. H. Li, X. M. Jiang, N. Cui, C. Yuan, S. F. Zhang, Q. B. Lu, Z. D. Yang, Q. L. Xin, Y. B. Song, X. A. Zhang, H. Z. Liu, J. Du, X. J. Fan, L. Yuan, Y. M. Yuan, Z. Wang, J. Wang, L. Zhang, D. N. Zhang, Z. B. Wang, K. Dai, J. Y. Bai, Z. N. Hao, H. Fan, L. Q. Fang, G. Xiao, Y. Yang, K. Peng, H. Q. Wang, J. X. Li, L. K. Zhang, W. Liu, Clinical effect and antiviral mechanism of T-705 in treating severe fever with thrombocytopenia syndrome. *Signal Transduct. Target. Ther.* **6**, 145 (2021).
38. A. A. Preobrazhensky, S. Dragan, T. Kawano, M. A. Gavrilin, I. V. Gulina, L. Chakravarty, P. E. Kolattukudy, Monocyte chemotactic protein-1 receptor CCR2B is a glycoprotein that has tyrosine sulfation in a conserved extracellular N-terminal region. *J. Immunol.* **165**, 5295–5303 (2000).
39. J. H. Y. Tan, J. P. Ludeman, J. Wedderburn, M. Canals, P. Hall, S. J. Butler, D. Taleski, A. Christopoulos, M. J. Hickey, R. J. Payne, M. J. Stone, Tyrosine sulfation of chemokine receptor CCR2 enhances interactions with both monomeric and dimeric forms of the chemokine monocyte chemoattractant protein-1 (MCP-1). *J. Biol. Chem.* **288**, 10024–10034 (2013).
40. A. K. Apel, R. K. Y. Cheng, C. S. Tautermann, M. Brauchle, C. Y. Huang, A. Pautsch, M. Hennig, H. Nar, G. Schnapp, Crystal structure of CC chemokine receptor 2A in complex with an orthosteric antagonist provides insights for the design of selective antagonists. *Structure* **27**, 427–438.e5 (2019).
41. A. Bourmaud, S. Gallien, B. Domon, Parallel reaction monitoring using quadrupole-Orbitrap mass spectrometer: Principle and applications. *Proteomics* **16**, 2146–2159 (2016).
42. S. Li, H. Li, Y. L. Zhang, Q. L. Xin, Z. Q. Guan, X. Chen, X. A. Zhang, X. K. Li, G. F. Xiao, P. Y. Lozach, J. Cui, W. Liu, L. K. Zhang, K. Peng, SFTSV Infection Induces BAK/BAX-dependent mitochondrial DNA release to trigger NLRP3 inflammasome activation. *Cell Rep.* **30**, 4370–4385.e7 (2020).
43. S. F. Zhang, Z. D. Yang, M. L. Huang, Z. B. Wang, Y. Y. Hu, D. Miao, K. Dai, J. Du, N. Cui, C. Yuan, H. Li, X. K. Li, X. A. Zhang, P. H. Zhang, X. M. Mi, Q. B. Lu, W. Liu, Preexisting chronic conditions for fatal outcome among SFTS patients: An observational cohort study. *PLOS Negl. Trop. Dis.* **13**, e0007434 (2019).
44. T. U. Metcalf, P. A. Wilkinson, M. J. Cameron, K. Ghneim, C. Chiang, A. M. Wertheimer, J. B. Hiscott, J. Nikolich-Zugich, E. K. Haddad, Human monocyte subsets are transcriptionally and functionally altered in aging in response to pattern recognition receptor agonists. *J. Immunol.* **199**, 1405–1417 (2017).
45. S. Mine, Y. Okada, T. Tanikawa, C. Kawahara, T. Tabata, Y. Tanaka, Increased expression levels of monocyte CCR2 and monocyte chemoattractant protein-1 in patients with diabetes mellitus. *Biochem. Biophys. Res. Commun.* **344**, 780–785 (2006).
46. T. Suzuki, Y. Sato, K. Sano, T. Arashiro, H. Katano, N. Nakajima, M. Shimojima, M. Kataoka, K. Takahashi, Y. Wada, S. Morikawa, S. Fukushi, T. Yoshikawa, M. Saijo, H. Hasegawa, Severe fever with thrombocytopenia syndrome virus targets B cells in lethal human infections. *J. Clin. Invest.* **130**, 799–812 (2020).
47. E. S. Park, M. Shimojima, N. Nagata, Y. Ami, T. Yoshikawa, N. Iwata-Yoshikawa, S. Fukushi, S. Watanabe, T. Kurosu, M. Kataoka, A. Okutani, M. Kimura, K. Imaoka, K. Hanaki, T. Suzuki, H. Hasegawa, M. Saijo, K. Maeda, S. Morikawa, Severe fever with thrombocytopenia syndrome *Phlebovirus* causes lethal viral hemorrhagic fever in cats. *Sci. Rep.* **9**, 11990 (2019).
48. Z. Li, C. Bao, J. Hu, C. Gao, N. Zhang, H. Xiang, C. J. Cardona, Z. Xing, Susceptibility of spotted doves (*Streptopelia chinensis*) to experimental infection with the severe fever with thrombocytopenia syndrome phlebovirus. *PLOS Negl. Trop. Dis.* **13**, e0006982 (2019).

49. Y. Sun, Y. Qi, C. Liu, W. Gao, P. Chen, L. Fu, B. Peng, H. Wang, Z. Jing, G. Zhong, W. Li, Nonmuscle myosin heavy chain IIA is a critical factor contributing to the efficiency of early infection of severe fever with thrombocytopenia syndrome virus. *J. Virol.* **88**, 237–248 (2014).
50. R. K. Jangra, A. S. Herbert, R. Li, L. T. Jae, L. M. Kleinfelter, M. M. Slough, S. L. Barker, P. Guardado-Calvo, G. Roman-Sosa, M. E. Dieterle, A. I. Kuehne, N. A. Muena, A. S. Wirchnianski, E. K. Nyakatura, J. M. Fels, M. Ng, E. Mittler, J. Pan, S. Bharrhan, A. Z. Wec, J. R. Lai, S. S. Sidhu, N. D. Tischler, F. A. Rey, J. Moffat, T. R. Brummelkamp, Z. Wang, J. M. Dye, K. Chandran, Protocadherin-1 is essential for cell entry by New World hantaviruses. *Nature* **563**, 559–563 (2018).
51. M. Kimura, K. Egawa, T. Ozawa, H. Kishi, M. Shimojima, S. Taniguchi, S. Fukushi, H. Fujii, H. Yamada, L. Tan, K. Sano, H. Katano, T. Suzuki, S. Morikawa, M. Saijo, H. Tani, Characterization of pseudotyped vesicular stomatitis virus bearing the heartland virus envelope glycoprotein. *Virology* **556**, 124–132 (2021).
52. Y. Zhang, S. Shen, J. Shi, Z. Su, M. Li, W. Zhang, M. Li, Z. Hu, C. Peng, X. Zheng, F. Deng, Isolation, characterization, and phylogenic analysis of three new severe fever with thrombocytopenia syndrome bunyavirus strains derived from Hubei Province, China. *Virol. Sin.* **32**, 89–96 (2017).
53. L. K. McMullan, S. M. Folk, A. J. Kelly, A. MacNeil, C. S. Goldsmith, M. G. Metcalfe, B. C. Batten, C. G. Albarino, S. R. Zaki, P. E. Rollin, W. L. Nicholson, S. T. Nichol, A new phlebovirus associated with severe febrile illness in Missouri. *N. Engl. J. Med.* **367**, 834–841 (2012).
54. S. Li, X. Zhu, Z. Guan, W. Huang, Y. Zhang, J. Kortekaas, P. Y. Lozach, K. Peng, NSs filament formation is important but not sufficient for RVFV virulence In Vivo. *Viruses* **11**, 834 (2019).
55. Y. Zhang, B. H. Liu, F. Lin, Y. G. Zhang, B. Y. Si, X. P. Kang, Y. Hu, J. Li, X. Y. Wu, Y. C. Li, Q. Y. Zhu, Y. H. Yang, The first complete genomic characterization of an Amur virus isolate from China. *Arch. Virol.* **158**, 2185–2188 (2013).

Acknowledgments

Funding: The study was supported by the National Key Research and Development Program of China (2021YFC2300200-02 to W.L.; 2018YFE0200401 to H.L.; 2021YFC2300700 to Leike Zhang; and 2022YFC2303300 to H.L., Leike Zhang, and K.P.), the National Natural Science Foundation of China (82172270 and 81722041 to H.L., 81825019 to W.L., 31970165 to Leike Zhang, and 32070179 to K.P.), and the Strategic Priority Research Program of the Chinese Academy of Sciences (XDB29010204 to K.P.). **Author contributions:** Conceptualization: W.L., H.L., L.-K.Z., and K.P. Methodology: L.-K.Z., X.-F.P., Q.-X.W., J.L., S.-M.L., S.H., L.-Y.Z., and H.D. Investigation: J.L., Q.-X.W., S.H., L.-Y.Z., and X.-G.D. Supervision: K.P., C.-Y.W., and G.-F.X. Writing original draft: H.L., W.L., L.-K.Z., and K.P. Writing—review and editing: H.L., W.L., L-K.Z., and K.P. **Competing interests:** The authors declare that they have no competing interests. **Data and materials availability:** All data needed to evaluate the conclusions in the paper are present in the paper and/or the Supplementary Materials.

Submitted 14 January 2023
Accepted 30 June 2023
Published 2 August 2023
10.1126/sciadv.adg6856